*Desalination and Water Treatment*
www.deswater.com
doi: 10.1080/19443994.2013.873352

53 (2015) 3482–3490
March

Taylor & Francis
Taylor & Francis Group

# Ultrapure water from seawater using integrated reverse osmosis-capacitive deionization system

Y.A.C. Jande[a,b,1], M.B. Minhas[a,1], W.S. Kim[a,*]

[a]*Department of Mechanical Engineering, Hanyang University, 55 Hanyangdaehak-ro, Sangnok-gu, Kyeonggi-do, Ansan 426-791, Korea*
*Tel. +82 31 400 5248; Fax: +82 31 418 0153; email: wskim@hanyang.ac.kr*
[b]*Department of Materials Science and Engineering, Nelson Mandela African Institution of Science and Technology, Arusha, Tanzania*

Received 2 July 2013; Accepted 4 December 2013

ABSTRACT

The use of water for particular application depends on its purity level. In accordance with the world health organization, water with total dissolved salts (TDS) less than 500 ppm can be considered good for human consumption. Ultrapure water is used in areas such as semiconductor industry, pharmaceuticals, and laboratories. Purification processes like electrodeionization process, thermal processes, and membrane processes are used to produce ultrapure water from very low salinity (10–200 ppm) water source. In this study, seawater is desalinated to produce ultrapure water using the integrated reverse osmosis (RO)-capacitive deionization (CDI). The RO permeate is fed to the CDI cell to generate the high purity water. It has been found that, with the use of RO-CDI integrated system, seawater can be used to produce ultrapure water with TDS less than 2 ppm and potable water with TDS less than 400 ppm by consuming 3.171 kWh/m$^3$ of energy. The proposed integrated RO-CDI system is of significant interest in the areas where ultrapure water along with fresh water is required from seawater.

*Keywords:* Reverse osmosis; Capacitive deionization; Seawater; Ultrapure water; Desalination

## 1. Introduction

Water is one of the fundamental needs of human life. The demand of clean water for various applications such as industrial, domestic, and agricultural use is increasing with population. Water from different sources like underground water, seawater, and waste water from industries have different percentage of salts/impurities and thus can be classified on the basis of mixed salts. In Lindahl et al. [1], the authors have classified the water as natural, deionized, distilled, and ultra-clean based on the dissolved impurities. The natural water ranges from naturally occurring contaminated to potable water. In the deionized water, salts/minerals are absent. By distilling the inorganic, organic, and ionic, contamination is removed from water. The ultraclean water is degassed and is free of salts, metals, and lime. The conductivity of seawater is

*Corresponding author.

[1]Equally contributed.

~5 S/m, drinking water is 5–50 mS/m, and of high purity is about 5.5 μS/m [1]. The pure water is considered as a poor conductor, but impure/domestic water is considered as a good conductor. The conductivity ratio of seawater, potable water, and ultrapure water is 1,000,000:1,000:1 [2].

The water quality technical standards have been established by many professional organizations, including the American Chemical Society, American Society for testing and Materials (ASTM), the US National Committee for Clinical Laboratory Standards (NCCLS) now called Clinical and Laboratory Standards Institute, European Pharmacopeia (EP), and the United States Pharmacopeia (USP) [2]. The different categorizes of ultrapure water by standardizing organizations are presented in Table 1.

The tap water meets most liquid cooling requirements in industry, but the applications such as laser cutting, laboratory instrumentation, pharmaceutical, cosmetics, food processing, semiconductor manufacturing, plating, and other chemical processing require deionized (DI) water. The chemical and electrical properties of DI water make it suitable for cooling the sensitive electronics [3]. DI water is highly reactive, so the materials of distribution piping and storage vessels leach out. It has poor taste and lack beneficial minerals for human health and not recommended for drinking [4].

Ultrapure water is usually produced using desalination technologies such as distillation processes, membrane desalination processes, and electrodeionization (EDI). For the distillation processes, energy consumption is independent of the feed concentration. Distillation processes such as multi-stage flash distillation, multi-effect distillation, mechanical vapor compression, and thermal vapor compression consume about 19.58–27.25, 14.45–21.35, 7.00–12.00, and 16.26 kWh/m$^3$, respectively. Also, seawater reverse osmosis (SWRO) with energy recovery, brackish water reverse osmosis (BWRO) with energy recovery, and electrodialysis (ED) utilizes 4.00–6.00, 1.50–2.50, and 0.70–5.50 kWh/m$^3$, respectively, in which the water quality by SWRO is 400–500 ppm, BWRO is 200–500 ppm, and ED is 150–500 ppm [5].

Through the use of ED, the author in reference [6] reported the production of ultrapure water (6 μS/cm ≈ 3.84 ppm) from tap water (175.6 μS/cm ≈ 122 ppm), but there is the problem of concentration polarization. EDI utilizes the advantages of ED and ion-exchange resins to produce ultrapure water with the resistivity between 1 and 18 MΩ cm [7,8]. However, EDI has the disadvantages such as partial difference in resin regeneration caused by uneven current flow and the

Table 1
A comparative presentation of different quality standards for ultrapure water [2]

| | | ISO 3696 (1987) | | | ASTM (D1193–91) | | | | NCCLS (1988) | | | Pharmacopoeia | |
|---|---|---|---|---|---|---|---|---|---|---|---|---|---|
| Contaminant | Parameter | Grade 1 | Grade 2 | Grade 3 | Type I* | Type II* | Type III* | Type IV | Type I | Type II | Type III | EP (20°C) | USP |
| Ions | Resistivity at 25°C (MΩ cm) | 10 | 1 | 0.2 | 18 | 10 | 4 | 0.2 | >10 | >1 | >0.1 | >0.23 | >0.77 |
| | Conductivity at 25°C (μS cm$^{-1}$) | 0.1 | 1 | 5 | 0.056 | 0.1 | 0.25 | 5 | <0.1 | <1 | <10 | <4.3 | <1.3 |
| Acidity/alkalinity | pH at 25°C | – | – | 5.0–7.5 | – | – | – | 5.0–8.0 | – | – | 5.0–8.0 | – | – |
| Organics | Total organic carbon/ppb (μg/L) | – | – | – | 50 | 50 | 200 | – | <50 | <200 | <1,000 | <500 | <500 |
| Total solids | mg/kg | – | 1 | 2 | – | – | – | – | 0.1 | 1 | 5 | – | – |
| Colloids | Silica (μg/mL) | – | – | – | <2 | <3 | <500 | – | <0.05 | <0.1 | <1 | – | – |
| Bacteria | CFU/mL | – | – | – | – | – | – | – | <10 | <1,000 | – | <100 | <100 |

treated water can be contaminated by ions which are transported back to the feed (diluate) compartment due to the incomplete permselectivity of ion-exchange membranes [9]. The incomplete permselectivity can be resolved by using bipolar membranes [7,10], Lee and Choi [9] describes the demerits of bipolar membranes as there is an increase in EDI structural complexity. Furthermore, Lee and Choi [9] uses membrane capacitive deionization (MCDI) technology to produce ultrapure water with resistivity of 2–9 MΩ cm from feed water of ~20.2 μS/cm. However, the resistivity values reported by this author are the instantaneous lowest effluent concentration. The pooled purified water normally has lower purity than the lowest effluent concentration for the MCDI/capacitive deionization (CDI) charged at constant voltage [11]. Also, continuous electrodeionization (CEDI) is widely used in producing ultrapure water. The typical feed concentration for the CEDI system is 25–50 μS/cm (16–32 ppm) in which 0.25 kWh/m$^3$ of power is used in ultrapure water production [12]. In Desale et al. [13], the author performed experiments using the vertical multiple effect distillation unit to produce distilled water with output concentration 7.93 and 17.12 ppm while their feed water was tap water (530 ppm) and low-salinity pretreated seawater (18,000 ppm), respectively.

The production of ultrapure water from ordinary tap water/low-concentration potable water was already studied by many researchers such as [7,9]. The authors were unable to find any published work to obtain ultrapure water from seawater. Therefore, the production of ultrapure water from seawater is studied and energy requirements are estimated. A common approach in seawater desalination is using reverse osmosis (RO). RO is a pressure-driven process for removing salts from water using semi-permeable membranes allowing selective flow of water through it. Over a billion gallon/day of water is desalted by RO [14]. Different RO elements/modules were designed to maintain high performance of membranes. Spiral wound module is widely used membrane module than other modules like hollow fiber, and tubular types [14–16]. In RO, the inclusion of energy recovery device (ERD) is also important and published work in the area of energy recovery is abundant such as [17–20]. RO technology is fully developed/commercial, while CDI is the emerging desalination technology for desalting saline water. CDI is generally comprised of pair/pairs of electrodes in which between the electrodes there is a spacer. During purification process, the electric voltage is applied to polarize the electrodes—one electrode becomes positively charged and the other electrode becomes negatively charged. The negative ions (anions) found in the saline water is attracted towards the positive electrode and the positive ions (cations) are attracted towards the negative electrode. The ions adsorption continues until porous electrodes ceases to adsorb more ions from the bulk stream, and then the supplied potential is either reversed or short-circuited to desorb ions from the porous electrodes to the saline stream. The regeneration process continues until the effluent concentration becomes equal to the influent concentration. To produce fresh water from seawater, many researchers have individually applied RO and/or CDI such as [21,22].

The fundamental strategy in desalination is the cost-effective production of water. A recent procedure of reducing energy consumption is by the integration of different desalination techniques [23,24]. In present study, the integration of RO and CDI is studied. Using the integrated/hybrid RO-CDI system, in present work, the production of ultrapure water from seawater is analyzed. Saline water is fed to RO and the RO permeate is passed through the CDI cell for further purification. Different feed salinities to the RO-CDI system are fed and the quantity of ultrapure water and potable water produced from the integrated system is computed along with corresponding energy requirement. The computed energy consumption in present work in comparison to the published energy requirements for seawater desalination is also presented.

## 2. Methodology

### 2.1. RO

In order to numerically estimate RO desalination phenomena, several numerical models are available in the literature. Based on different membrane/modules/applications, many researchers have proposed different models such as [16,22,25,26]. The typical outputs of RO model are the permeate flow rate/water production and the permeate concentration/salt rejection. In present work, (for RO), the seawater desalination experimental data [25] are simulated by published numerical model [16]. The model parameters used in the simulation are obtained from reference [16]. The fundamental equations of the model are summarized below:

The volumetric flux $J_v$ through the membrane is:

$$J_v = A[\Delta P - \sigma \Delta \pi] \quad (1)$$

where $A$ is the water permeability, $\Delta P$ is trans-membrane pressure, $\sigma$ is the reflection coefficient (dimensionless), and $\Delta\pi$ is the osmotic pressure difference across the membrane ($\pi = \alpha C$, where is the proportionality constant and $C$ is the solute concentration). During the desalination operation, the accumulation of salt on the membrane surface causes concentration difference between the feed stream and on the surface of membrane, which is accounted for by concentration polarization ($\Phi$) given by:

$$\Phi = \frac{C_m - C_p}{C_b - C_p} = \exp\left(\frac{J_v}{k}\right) \tag{2}$$

where $k$ is the mass transfer coefficient and subscript $m$ represents the membrane feed interface, $p$ is the permeate side, and $b$ is the brine side. The permeate concentration can be calculated as follows:

$$C_p = \left(\frac{\Phi(1-R)C_b}{\Phi + R(1-\Phi)}\right) \tag{3}$$

where $R$ is the percentage salt rejection expressed as:

$$R = \left(\frac{C_m - C_p}{C_m}\right) \times 100 \tag{4}$$

In addition to the simulation modeling, the following procedure was adopted to estimate the net energy consumption by RO.

Specific energy consumption ($\mathrm{SEC_{RO}}$) is:

$$\mathrm{SEC_{RO}} = \frac{\dot{W}}{Q_p} \tag{5}$$

where $Q_p$ is the permeate flow rate and the pump work $\dot{W}$ is given as:

$$\dot{W} = \frac{Q_f \Delta P^*}{\eta_p} \tag{6}$$

where $Q_f$ is the flow rate, the pressure difference between the suction and discharge of pump is $\Delta P^*$, and $\eta_p$ is the pump efficiency (assumed $\eta_p$= 0.9).

The brine stream exiting RO module carries pressure energy and energy recovered ($E_{\mathrm{ERD}}$) by an ERD is [27]:

$$E_{\mathrm{ERD}} = P_b\left(\frac{Q_f}{Q_p} - 1\right)\eta_{\mathrm{ERD}} \tag{7}$$

where $P_b$ is the brine pressure at exit of RO module and $\eta_{\mathrm{ERD}}$ is the efficiency of ERD (assumed $\eta_{\mathrm{ERD}}$ = 0.9).

The net specific energy consumption by RO is given as:

$$\mathrm{SEC_{Net-RO}} = \mathrm{SEC_{RO}} - E_{\mathrm{ERD}} \tag{8}$$

### 2.2. Capacitive deionization (CDI)

The CDI operating parameters such as dead volume, flow rate, resistance, capacitance, applied potential, and spacer volume for the desired effluent concentration are found using the model and procedure described in reference [21]; the model important details are described below.

The lowest concentration is:

$$C_{\mathrm{alowest}} = C_f - \frac{\mu}{V_s} y^x [1 - y] \tag{9}$$

where

$$x = \frac{V_c}{\phi R_{\mathrm{series}} C_a}$$

$$y = \frac{V_c}{V_c + \phi R_{\mathrm{series}} C_a}$$

$$\mu = \frac{\varepsilon C_a V}{zF}\left(1 - e^{-\frac{V_s}{\phi R_{\mathrm{series}} C_a}}\right)$$

$$\alpha = \frac{1}{R_{\mathrm{series}} C_a}, \quad \beta = \frac{1}{R_{\mathrm{series}} C_a} + \frac{\phi}{V_c}$$

$C_f$: feed concentration, $V_s$: spacer volume, $\varepsilon$: Coulombic efficiency, $C_a$: capacitance, $V$: applied voltage, $z$: averaged partial molar ionic valences of the feed solution, $F$: Faraday's constant, $\phi$: flow rate, $V_c$: dead volume, and $R_{\mathrm{series}}$: series resistance. The corresponding lowest concentration time is:

$$t_{\mathrm{alcef}} = \frac{V_c}{\phi} \ln\left(1 + \frac{\phi R_{\mathrm{series}} C_a}{V_c}\right) \tag{10}$$

The time in which the CDI cell attains its lowest effluent concentration is known as the *lowest concentration time* and the corresponding effluent concentration is known as *lowest concentration.* Genetic algorithm is used to find out the CDI parameters to achieve the desired lowest concentration. The details of this methodology are explained in Jande and Kim [21].

The transient behavior of the CDI cell during adsorption and desorption can be described by the following equations:

Effluent concentration during adsorption is:

$$C_{\mathrm{ef}}(t) = C_f - \frac{\mu}{V_s}(e^{-\alpha t} - e^{-\beta t}) \tag{11}$$

and the effluent concentration during desorption is:

$$C(t) = C_f - \frac{\mu_d}{V_s}(\rho_1 e^{-\beta t} - \rho_2 e^{-\alpha t}) \tag{12}$$

where

$$\mu_d = \frac{1.3\varepsilon C_a(V_{\mathrm{cap}} - V_{\mathrm{d}})}{zF}\left(1 - e^{-\frac{V_s}{\phi R_{\mathrm{series}} C_a}}\right)$$

$$\rho_1 = e^{\beta t_{\mathrm{eq}}}, \rho_2 = e^{\alpha t_{\mathrm{eq}}}$$

and $V_d$: the voltage applied during discharging. $V_{\mathrm{cap}}$: CDI cell charge potential for the duration of $t_{\mathrm{eq}}$, and $V_{\mathrm{cap}}$ is:

$$V_{\mathrm{cap}} = V\left(1 - e^{-\frac{t_{\mathrm{eq}}}{R_{\mathrm{series}} C_a}}\right) \tag{13}$$

The pooled purified water has the purity level to be found using the following equation:

$$C_t = \frac{1}{t_2 - t_1 + 1}\int_{t_1}^{t_2} C_{ef}(t)\mathrm{d}t \tag{14}$$

where $t_1$ is the pooling starting time and $t_2$ is the pooling final time. In CDI cell, the total amount of pure water is found by considering the pooling time and the flow rate, and it can be computed using the following formula:

$$\mathrm{APW}_{\mathrm{CDI}} = (t_2 - t_1 + 1)\phi \tag{15}$$

The amount of brackish water or saline water passed through the CDI for purification within one cycle is

$$\mathrm{AB} = t_c\phi \tag{16}$$

where $t_c$ is the cycle time.

Neglecting the energy dissipation due to the resistance, the specific energy consumption used to produce the given amount of pure water using CDI cell is:

$$\mathrm{SEC}_{\mathrm{CDI}} = \frac{C_a \times V_{\mathrm{cap}}^2}{2 \times \mathrm{APW}} \tag{17}$$

### 2.3. RO-CDI hybrid system

The flow diagram for integrated RO-CDI system to produce ultrapure water from seawater is presented in Fig. 1. The output of the RO-CDI system is ultrapure water in addition to fresh/potable water. Seawater is fed to RO module, and the output permeate stream from RO is fed to CDI for further salt removal. In order to obtain the optimum operating conditions, the simulation model for spiral wound module was integrated with optimization software PIAnO (Process Integration, Automation and Optimization) [28]. The variables set for this optimization problem were the feed conditions such as pressure and flow rate. For this unconstrained optimization, the minimization of SEC (Eq. (5)) was set as the objective function. Subsequently, using the numerical model at the optimum feed conditions, the permeate flow rate and permeate concentration were determined. The procedure to estimate the quantity of desalinated water along with its salt concentration using CDI is already explained in previous section.

The effect of different feed concentrations on the production of ultrapure water, water purity, and energy requirement was also studied. The quantity of

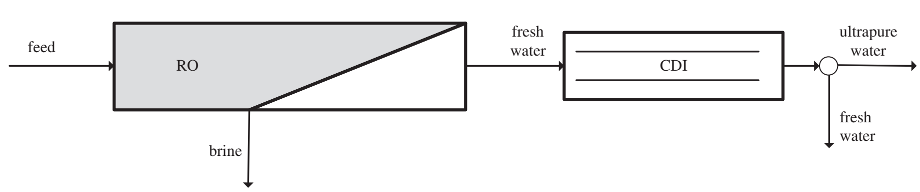


Fig. 1. Schematic diagram of RO-CDI hybrid system to produce ultrapure/potable water from seawater.

fresh water produced in one CDI cycle time ($t_c$) is $Q_{\mathrm{RO}}$ calculated as:

$$Q_{\mathrm{RO}} = q_p t_c \tag{18}$$

where $q_p$ is the RO permeate flow rate.

The total volume/amount of ultrapure water produced by integrated RO-CDI system is $\mathrm{APW}_{\mathrm{CDI}}$ and the amount of fresh water by the integrated system is:

$$Q_{R-\mathrm{CDI}} = Q_{\mathrm{RO}} - \mathrm{APW}_{\mathrm{CDI}} \tag{19}$$

The total energy consumed by the integrated RO-CDI system for the production of ultrapure water and fresh water from seawater is:

$$\mathrm{SEC}_T = \mathrm{SEC}_{\mathrm{Net-RO}} + \mathrm{SEC}_{\mathrm{CDI}} \tag{20}$$

## 3. Results and discussion

In the present study for producing ultrapure water from seawater, RO and CDI cell were incorporated. The water production and energy requirement from the proposed integrated RO and CDI system are discussed below.

In the RO experiment, three different artificial seawater solutions (sodium chloride solution (Instant Ocean)) were fed. The RO module used was 2.5 in. Filmtech FT 30 (thin film composite polyamide membrane). Further details of the module can be collected from references [16,29,30]. As explained in the previous Section, the optimum feed operating conditions for RO module were obtained by optimization. For optimization micro-genetic algorithm [31] was selected using standard optimization package (PIAnO). The variables/factors in this optimization problem were feed flow rate and feed pressure. The optimization range for variables was set within the range of experimental data (pressure 50–80 bar, flow rate 100–240 mL/s). In order to avoid the optimization problem to yield local minima, different initial conditions were tried to yield the same result. The determined optimum feed conditions along with the simulated permeate flow rate and concentration are summarized in Table 2. Three different feed concentrations (25,000, 35,000, and 40,000 ppm) were studied to understand the productivity of ultrapure water and cost. The optimum feed pressure increased with feed concentration and the permeate flow rate decreased with increasing concentration. The optimum feed flow rate for all three Cases is 100 mL/s (see Table 2).

Table 2
Optimum feed conditions and calculation results for RO

| Conditions | Case-I | Case-II | Case-III |
|---|---|---|---|
| Feed concentration (ppm) | 25,000 | 35,000 | 40,000 |
| Feed temperature (℃) | 25 | 25 | 25 |
| Feed pressure (bar) | 61 | 78 | 80 |
| Feed flow rate (mL/s) | 100 | 100 | 100 |
| Permeate flow rate (mL/s) | 20.946 | 19.968 | 17.978 |
| Permeate concentration (ppm) | 129.7 | 197.2 | 242.4 |
| Rejection (%) | 99.7 | 99.7 | 99.6 |
| $\mathrm{SEC}_{\mathrm{Net-RO}}$ (kWh/m$^3$) (Eq. (8)) | 3.161 | 4.184 | 4.55 |

It is evident from Eqs. (5)–(6) that SEC varies with feed pressure. The osmotic pressure is a function of feed water concentration; therefore, high salinity water has high osmotic pressure which requires high feed pressure in RO. Thus, the optimum pressure and $\mathrm{SEC}_{\mathrm{Net-RO}}$ presented in Table 2 increased with feed concentration. The resulting permeate from RO is fed to CDI cell as shown in Fig. 1, to produce ultrapure water.

The influent concentration in CDI cell is 129.7, 197.2, and 242.4 ppm. The corresponding CDI parameters to acquire ultrapure water using genetic algorithm: for 129.7 ppm are $V = 1.8$ V, $V_s = 20$ mL, $\phi$ = 20.946 mL/s, $C_a = 104$ F, $R_{\mathrm{series}} = 0.350\,\Omega$, and $V_c$ = 20 mL; for 197.2 ppm are $V = 2$ V, $V_s = 15$ mL, $\phi$ = 19.968 mL/s, $C_a = 205$ F, $R_{\mathrm{series}} = 0.285\,\Omega$, and $V_c = 15$ mL; and for 242.4 ppm are $V = 2$ V, $V_s = 15$ mL, $\phi$ = 17.978 mL/s, $C_a = 213$ F, $R_{\mathrm{series}} = 0.254\,\Omega$, and $V_c = 15$ mL. The CDI cell was discharged by applying zero voltage (short circuited).

The transient behavior of salt removal for the CDI cell possessing the above characteristics is shown in Fig. 2. During the CDI operation: for $C_f = 129.7$ ppm, the lowest concentration, 0.0867 ppm, is reached after 4 s; in which around 99.93% of the salt is removed, for $C_f = 197.2$ ppm, the lowest concentration is 0.0961 ppm (99.95% salt removal) reached after 3 s, and $C_f = 242.4$ ppm, the lowest concentration is 0.0712 ppm (99.97% salt removal) reached after 4 s. However, purified water is normally pooled into a tank for a specified period of time and has a purity level lower than that of the lowest effluent concentration. In this study, the pooled purified water has the total dissolved salts (TDS) of 1.567 ppm (2.450 μS/cm), 1.916 ppm (2.990 μS/cm), and 2.156 ppm (3.370 μS/cm) for $C_f$ = 129.7, 197.2, and 242.4 ppm, respectively, in which the purification time is 5 s for each case. The amount of ultrapure water in one cycle time is 105, 100, and 90 mL for $C_f = 129.7$, 197.2, and 242.4 ppm,

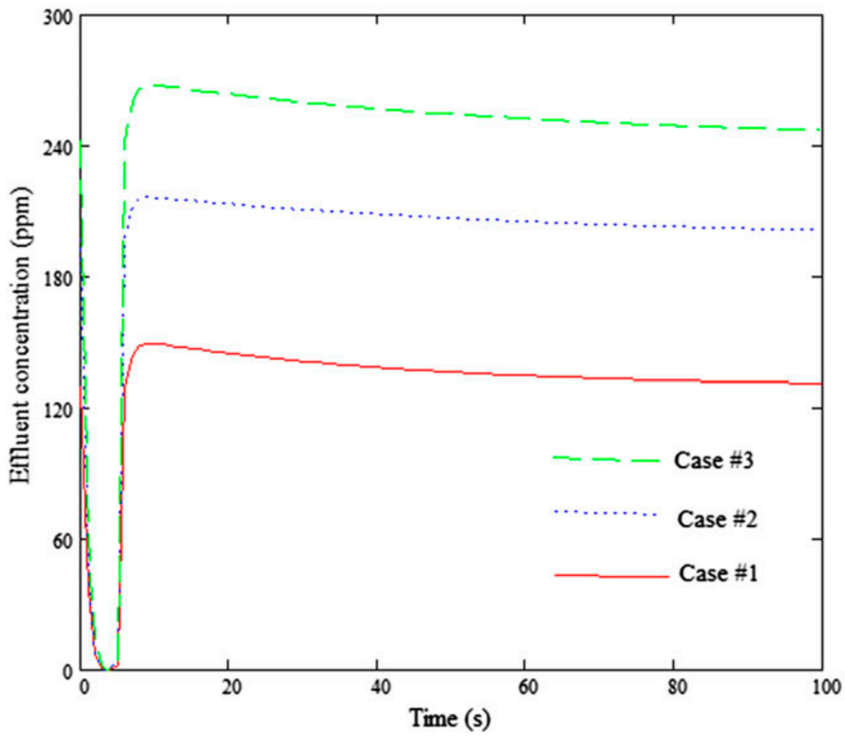


Fig. 2. The transient behavior of the CDI cell when set #1: $C_f = 129.7$ ppm, $V = 1.8$ V, $V_s = 20$ mL, $\phi = 20.946$ mL/s, $C_a = 104$ F, $R_{\text{series}} = 0.350\ \Omega$, and $V_c = 20$ mL, set #2: $C_f = 197.2$ ppm, $V = 2$ V, $V_s = 15$ mL, $\phi = 19.968$ mL/s, $C_a = 205$ F, $R_{\text{series}} = 0.285\ \Omega$, and $V_c = 15$ mL, and set #3: $C_f = 242.4$ ppm are $V = 2$ V, $V_s = 15$ mL, $\phi = 17.978$ mL/s, $C_a = 213$ F, $R_{\text{series}} = 0.254\ \Omega$, and $V_c = 15$ mL.

respectively, in which one cycle takes around 100 s for each case. The rest of water in this cycle can be used as drinking water, since they have TDS less than 400 ppm. CDI cell utilizes 0.010, 0.011, and 0.015 kWh/m$^3$ for $C_f = 129.7$, 197.2, and 242.4 ppm, respectively, of energy to produce ultrapure water.

In a commercial RO, many membrane elements (38) are used in single pressure vessel [32] and these pressure vessels are stacked in multi-pass and/or multi-stage arrangements to increase water recovery and reduce SEC. The water recovery in a commercial RO seawater desalination is normally over 30% [17]. In our present work, the analysis is based on single RO element with reasonable water recovery. The SEC is a normalized parameter (the energy consumed per unit of permeate produced) suitable for comparing different desalination systems with different water recoveries. The energy required to produce ultrapure water and fresh water via the integral RO-CDI cell can be obtained from Eq. (20)—which is 3.171, 4.195, and 4.565 kWh/m$^3$ when the feed concentration to the RO-CDI system is 25,000, 35,000, and 40,000 ppm, respectively. The SEC required to produce ultrapure water and fresh water from seawater is lower than the SEC required to produce only potable water using thermal processes [5]. In this integrated system during one cycle time, 1.987, 1.897, and 1.708 L when the feed concentration to the RO-CDI system is 25,000, 35,000, and 40,000 ppm, respectively, fresh water is produced in addition to the ultrapure water. Also, the feed concentration to CDI cell affects the SEC significantly as it can be seen in those three cases. This energy cost is of course different from the investment cost in which a company has to incur for the given project. Therefore, this novel idea to obtain both the ultrapure water and potable water at a time is significant/cost effective.

## 4. Conclusion

In this study the integration of RO and CDI has been investigated in order to produce ultrapure water and potable water simultaneously from seawater. Three cases have been examined: the first one is when the seawater concentration is 25,000 ppm, the second one is when the concentration is 35,000 ppm, and the last one is when the feed concentration to RO-CDI integrated system is 40,000 ppm. The ultrapure water was found to have the purity of 1.567 ppm (2.450 μS/cm), 1.916 ppm (2.990 μS/cm), and 2.156 ppm (3.370 μS/cm) when the feed concentration to the RO-CDI integration system is 25,000, 35,000, and 40,000 ppm, respectively; and generally the potable water from all three cases has the concentration less than 400 ppm, which is the acceptable quality according to the World Health Organization. The energy consumption in simultaneous production of ultrapure water and potable water from seawater is 3.171, 4.195, and 4.565 kWh/$m^3$ when seawater concentration is 25,000, 35,000, and 40,000 ppm, respectively. The energy consumption in the present study is relatively lower than that used to produce distilled water (~10 ppm) by thermal process [5]. Therefore, the proposed integrated RO-CDI system is of significant interest in the areas where ultrapure water along with fresh water is required from seawater. This paper excluded the investment cost of the given RO-CDI integrated system.

## List of symbols

| | | |
|---|---|---|
| $A$ | — | water permeability ($m^3\,m^{-2}s^{-1}\,Pa^{-1}$) |
| AB | — | total amount of saline water passed through CDI in one cycle (mL) |
| $APW_{CDI}$ | — | amount of pure water from CDI (mL) |
| $C_a$ | — | CDI capacitance (F) |
| $C_{alowest}$ | — | lowest concentration ($mg\,L^{-1}$) |
| $C_b$ | — | Brine concentration ($kg\,m^{-3}$) |
| $C_{ef}$ | — | effluent concentration in CDI (s) |
| $C_f$ | — | feed concentration in CDI ($mg\,L^{-1}$) |
| $C_m$ | — | feed concentration on membrane feed interface ($kg\,m^{-3}$) |
| $C_p$ | — | permeate concentration ($kg\,m^{-3}$) |
| $C_t$ | — | concentration of pooled purified water ($mg\,L^{-1}$) |
| ERD | — | energy recovery device |
| $E_{ERD}$ | — | energy recovered by ERD ($kWh\,m^{-3}$) |
| $F$ | — | Faraday's constant |
| $J_v$ | — | volumetric flux ($m^3\,s^{-1}$) |
| $k$ | — | mass transfer coefficient ($ms^{-1}$) |
| $P_b$ | — | Brine pressure (Pa) |
| $\Delta P$ | — | trans-membrane pressure (Pa) |
| $\Delta P^*$ | — | pressure difference between suction and discharge of pump (Pa) |
| $Q_f$ | — | feed flow rate ($m^3\,s^{-1}$) |
| $Q_p$ | — | permeate flow rate ($m^3\,s^{-1}$) |
| $Q_{RO}$ | — | amount of fresh water produced by RO in one CDI cycle time (L) |
| $Q_{R\text{-}CDI}$ | — | fresh water produce by integrated RO-CDI system (L) |
| $R$ | — | rejection |
| $R_{series}$ | — | series resistance (Ω) |
| $SEC_{CDI}$ | — | specific energy consumption in CDI ($kWh\,m^{-3}$) |
| $SEC_{Net-RO}$ | — | net specific energy consumption in RO ($kWh\,m^{-3}$) |
| $SEC_{RO}$ | — | specific energy consumption in RO ($kWh\,m^{-3}$) |
| $SEC_T$ | — | total specific energy consumption by integrated RO-CDI system ($kWh\,m^{-3}$) |
| $t$ | — | time (s) |
| $t_{alcef}$ | — | lowest concentration time (s) |
| $t_{eq}$ | — | equilibrium time (s) |
| $t_c$ | — | cycle time (s) |
| $t_1$ | — | pooling starting time (s) |
| $t_2$ | — | pooling final time (s) |
| $V$ | — | applied voltage (V) |
| $V_c$ | — | dead volume (mL) |
| $V_{cap}$ | — | CDI cell charged potential (V) |
| $V_d$ | — | applied voltage during desorption (V) |
| $V_s$ | — | spacer volume (mL) |
| $\dot{W}$ | — | pump work (kW) |
| $z$ | — | molar fraction |
| $\phi$ | — | flow rate in CDI ($mL\,s^{-1}$) |
| $\varepsilon$ | — | coulumbic efficiency |
| $\sigma$ | — | reflection coefficient |
| $\Delta\pi$ | — | osmotic pressure difference across the membrane (Pa) |
| $\Phi$ | — | concentration polarization |
| $\eta_p$ | — | pump efficiency |
| $\eta_{ERD}$ | — | ERD efficiency |

## References


[1] M. Lindahl, N. Svensson, B.H. Svensson, E. Sundin, Industrial cleaning with qlean water—A case study of printed circuit boards, J. Cleaner Prod. 47 (2013) 19–25.

[2] Purified Water, in Wikipedia, the free encyclopedia, 2013.

[3] Deionized Water, Lytron Inc., USA, 2012.

[4] Nutrients in Drinking Water, WHO, Geneva, Switzerland, 2005.

[5] A. Al-Karaghouli, L.L. Kazmerski, Energy consumption and water production cost of conventional and renewable-energy-powered desalination processes, Renew. Sust. Energy Rev. 24 (2013) 343–356.

[6] A. Abou-Shady, H. Xu, C. Peng, Production of pure water suitable for laboratory experiments by electrodialysis technology, in: 5th International Conference on Bioinformatics and Biomedical Engineering (iCBBE), IEEE, Wuhan, 2011, pp. 1–4.

[7] A. Grabowski, G. Zhang, H. Strathmann, G. Eigenberger, The production of high purity water by continuous electrodeionization with bipolar membranes: Influence of the anion-exchange membrane permselectivity, J. Membr. Sci. 281 (2006) 297–306.

[8] T. Franken, Ultrapure water: More than membrane technology alone, Membr. Technol. (1999) 9–12.

[9] J.-H. Lee, J.-H. Choi, The production of ultrapure water by membrane capacitive deionization (MCDI) technology, J. Membr. Sci. 409–410 (2012) 251–256.

[10] A. Grabowski, G. Zhang, H. Strathmann, G. Eigenberger, Production of high-purity water by continuous electrodeionization with bipolar membranes: Influence of concentrate and protection compartment, Sep. Purif. Technol. 60 (2008) 86–95.

[11] R. Zhao, P. Biesheuvel, A. van der Wal, Energy consumption and constant current operation in membrane capacitive deionization, Energy Environ. Sci. 5 (2012) 9520–9527.
[12] J. Wood, J. Gifford, J. Arba, M. Shaw, Production of ultrapure water by continuous electrodeionization, Desalination 250 (2010) 973–976.
[13] G. Desale, P. Vasudevan, J. Pothal, K. Zala, B. Bhatti, S. Singh, P. Sen, Purification of water using vertical multiple effect distillation unit, J. Sci. Ind. Res. 70 (2011) 634–638.
[14] R.W. Baker, Membrane Technology and Applications, 2nd ed., John Wiley & Sons, 2004.
[15] E. Drioli, L. Giorno (Eds.), Comprehensive Membrane Science and Engineering, 1st ed., Academic Press (Elsevier), Oxford, 2010.
[16] S. Senthilmurugan, A. Ahluwalia, S.K. Gupta, Modeling of a spiral-wound module and estimation of model parameters using numerical techniques, Desalination 173 (2005) 269–286.
[17] A.M. Farooque, A.T.M. Jamaluddin, A.R. Al-Reweli, P.A.M. Jalaluddin, S.M. Al-Marwani, A.A. Al-Mobayed, A.H. Qasim, Parametric analyses of energy consumption and losses in SWCC SWRO plants utilizing energy recovery devices, Desalination 219 (2008) 137–159.
[18] A.O. Sharif, A.A. Merdaw, H. Al-Bahadili, A. Al-Taee, S. Al-Aibi, Z. Rahal, G.A.W. Derwish, A new theoretical approach to estimate the specific energy consumption of reverse osmosis and other pressure-driven liquid-phase membrane processes, Desalin. Water Treat. 3 (2009) 111–119.
[19] G. Migliorini, E. Luzzo, Seawater reverse osmosis plant using the pressure exchanger for energy recovery: A calculation model, Desalination 165 (2004) 289–298.
[20] L.F. Greenlee, D.F. Lawler, B.D. Freeman, B. Marrot, P. Moulin, Reverse osmosis desalination: Water sources, technology, and today's challenges, Water Res. 43 (2009) 2317–2348.
[21] Y.A.C. Jande, W.S. Kim, Predicting the lowest effluent concentration in capacitive deionization, Sep. Purif. Technol. 115 (2013) 224–230.
[22] P.P. Mane, P.-K. Park, H. Hyung, J.C. Brown, J.-H. Kim, Modeling boron rejection in pilot- and full-scale reverse osmosis desalination processes, J. Membr. Sci. 338 (2009) 119–127.
[23] W. Li, W.B. Krantz, E.R. Cornelissen, J.W. Post, A.R.D. Verliefde, C.Y. Tang, A novel hybrid process of reverse electrodialysis and reverse osmosis for low energy seawater desalination and brine management, Appl. Energy 104 (2013) 592–602.
[24] G. Calì, E. Fois, A. Lallai, G. Mura, Optimal design of a hybrid RO/MSF desalination system in a non-OPEC country, Desalination 228 (2008) 114–127.
[25] M.B. Boudinar, W.T. Hanbury, S. Avlonitis, Numerical simulation and optimisation of spiral-wound modules, Desalination 86 (1992) 273–290.
[26] S. Sundaramoorthy, G. Srinivasan, D.V.R. Murthy, An analytical model for spiral wound reverse osmosis membrane modules: Part I—Model development and parameter estimation, Desalination 280 (2011) 403–411.
[27] J.C. Van Dijk, P.J. De Moel, H.A. Van Den Berkmortel, Optimizing design and cost of seawater reverse osmosis systems, Desalination 52 (1984) 57–73.
[28] PIAnO (Process Integration, Automation and Optimization) User's Manual, Version 3.3, PIDOTECH Inc., 2011.
[29] M.B. Boudinar, Performance Prediction and Optimisation of Spiral Wound Modules, University of Glasgow, 1991.
[30] DOW FILMTEC™, Membranes in, Dow Water & Process Solutions, Form No. 609-00350-0911.
[31] K. Krishnakumar, Micro-genetic Algorithms for Stationary and Non-stationary Function Optimization, in: 1989 Advances in Intelligent Robotics Systems Conference, International Society for Optics and Photonics, 1990, pp. 289–296.
[32] F. Vince, F. Marechal, E. Aoustin, P. Bréant, Multi-objective optimization of RO desalination plants, Desalination 222 (2008) 96–118.